Atmospheric Environment 48 (2012) 56–65

Contents lists available at SciVerse ScienceDirect

Atmospheric Environment

journal homepage: www.elsevier.com/locate/atmosenv

Optical properties and vertical extension of aged ash layers over the Eastern Mediterranean as observed by Raman lidars during the Eyjafjallajökull eruption in May 2010

A. Papayannis [a,*], R.E. Mamouri [a], V. Amiridis [b], E. Giannakaki [c], I. Veselovskii [d], P. Kokkalis [a], G. Tsaknakis [a], D. Balis [c], N.I. Kristiansen [e], A. Stohl [e], M. Korenskiy [d], K. Allakhverdiev [f], M.F. Huseyinoglu [f], T. Baykara [f]

[a] Laser Remote Sensing Laboratory, Physics Department, National Technical University of Athens, 15780 Zografou, Greece
[b] Institute for Space Applications and Remote Sensing, National Observatory of Athens, Athens, Greece
[c] Laboratory of Atmospheric Physics, Aristotle University of Thessaloniki, Thessaloniki, Greece
[d] Physics Instrumentation Center of General Physics Institute, Troitsk, Moscow Region, 142190, Russia
[e] Norwegian Institute for Air Research, Kjeller, Norway
[f] Marmara Research Centre (MRC)-Turkish Scientific and Technological Council (TUBITAK), Materials Institute, Gebze, Turkey

ARTICLE INFO

Article history:
Received 9 March 2011
Received in revised form
9 August 2011
Accepted 11 August 2011

Keywords:
Eyjafjallajökull
Optical properties of volcanic ash
Raman lidar
EARLINET
FLEXPART
HYSPLIT
BSC-DREAM8b

ABSTRACT

The vertical extension and the optical properties of aged ash layers advected from the Eyjafjallajökull volcanic eruption over the Eastern Mediterranean (Greece and Turkey) are presented for the period May 10–21, 2010. Raman lidar observations performed at three stations of EARLINET (Athens, Thessaloniki and Istanbul), provided clear ash signatures within certain layers, although ash was sometimes mixed with mineral dust advected from the Saharan region. AERONET columnar measurements did not indicate the presence of ash over the area for that period, although they did for the dust particles. This was further investigated and confirmed by simulations of the ash trajectories by the FLEXPART model and the BSC-DREAM8b dust model. Good agreement was found between simulated and observed geometrical characteristics of the ash and dust layers, respectively. Ash particles were observed over the lidar stations after 6–7-days transport from the volcanic source at height ranges between approximately 1.5 and 6 km. Mean ash particle layer thickness ranged between 1.5 and 2.5 km and the corresponding aerosol optical depth (AOD) was of the order of 0.12–0.06 at 355 nm and of 0.04–0.05 at 532 nm. Inside the ash layers, the lidar ratios (LR) ranged between 55 and 67 sr at 355 nm and 76–89 sr at 532 nm, while the particle linear depolarization ratio ranged between 10 and 25%.

1. Introduction

The eruption of the Eyjafjallajökull (63°38′N, 19°36′W, 1666 m above sea level-a.s.l.) volcano in Iceland during April and May 2010 was the largest in the last 1500 years and was characterized by magma of a slightly different composition than in earlier eruptions (Gudmundsson et al., 2010). The eruption started on April 14 and ended around May 19, 2010 (Showstack, 2010; Stohl et al., 2011). This volcanic activity led to an unprecedented disruption of the air traffic in Europe, and parts of the European air space were repeatedly closed in April and May. During the volcanic activity the London Volcanic Ash Advisory Center (VAAC) provided continuously updated reports (every 3–6 h) about ash dispersal over the European air space, thus alerting the aviation authorities on the presence of ash over the European continent. The total emitted ash mass was estimated to be of the order of 11.9 ± 5.9 Tg (Stohl et al., 2011). The eruption heights were found to be often of the order of 6–7 km but reached even heights of 10 km (Kaminski et al., in press; Stohl et al., 2011).

The episode was observed with a plethora of ground-based, airborne and space-borne instruments (Ansmann et al., 2010, 2011; Davies et al., 2010; Flentje et al., 2010; Markowicz et al., 2012; Nicolae et al., 2010; Sanderson, 2010; Dacre et al., 2011; Devenish et al., 2011; Gasteiger et al., 2011; Gross et al., 2011; Lettino et al., 2011; Matthias et al., 2012; Miffre et al., 2011; Revuelta et al., 2011; Schleicher et al., 2011; Schumann et al., 2011; Seifert et al., 2011; Wiegner et al., 2011). Similar observations were recently reported for the eruptions of Kasatochi and

* Corresponding author. Tel.: +30 210 7722992; fax: +30 210 7722928.
E-mail address: apdlidar@central.ntua.gr (A. Papayannis).

1352-2310/$ – see front matter © 2011 Elsevier Ltd. All rights reserved.
doi:10.1016/j.atmosenv.2011.08.037

Okmok volcanoes (Bitar et al., 2010; Corradini et al., 2010; Hoffmann et al., 2010; Karagulian et al., 2010; Mattis et al., 2010).

Satellite imagery and volcanic ash retrievals were used to monitor the ash transport, while reconnaissance research flights enabled direct monitoring of volcanic activity and the physico-chemical characterization of ash (Schumann et al., 2011). Moreover, the Lagrangian particle dispersion model FLEXPART was used in real time to predict the ash dispersion (Stohl et al., 2011). The 25 lidar stations of the European EARLINET lidar network followed the event almost continuously, and reported on the ash optical properties mostly close to the source region (Ansmann et al., 2010, 2011; Gasteiger et al., 2011; Nicolae et al., 2010). However, the optical properties of aged ash loads, in great distances from the volcano source are not presented in the literature.

In this paper we focus on the optical properties of the aged ash layers detected over the Eastern Mediterranean for the period of May 10–21, 2010. Section 2 of this paper presents the instruments and methods used in this study to follow the ash and mixed dust clouds and study their optical properties and vertical extension (Raman lidars, FLEXPART and HYSPLIT dispersion models and BSC-DREAM8b dust model). Section 3 presents a qualitative description of the ash plume dispersion over Europe, along with a brief overview of the vertical aerosol structure in conjunction with the optical properties and the total loadings of ash particles over the Eastern Mediterranean region, in occasional presence of dust particles. Finally, Section 4 presents our conclusions.

2. Instrumentation and methods

2.1. Raman lidar systems

All three Raman lidar systems (two in Greece and one in Turkey) (see Table 1) used in this study of the Eyjafjallajökull eruption are part of the EARLINET European aerosol monitoring network (Bösenberg et al., 2003). The lidar systems in Greece are located in Athens and Thessaloniki and they are run by the National Technical University of Athens (NTUA) and the Aristotle University of Thessaloniki (AUTH), respectively. Technical specifications of the lidar systems are given in Mamouri et al. (2009) for the Athens' lidar and in Giannakaki et al. (2010) for the Thessaloniki's one. The third EARLINET lidar is located at Gebze (Turkey, south-western of the city of Istanbul) and is run by the Marmara Research Center (MRC) (Allakhverdiev et al., 2009). All Raman lidars are based on Nd:YAG pulsed lasers (Table 1), emit at 355 and 532 nm and are equipped with a nitrogen (N_2) Raman channel (at 387 nm and 607 nm) to provide accurate profiling of the aerosol backscatter and extinction coefficients at 355 nm and 532 nm, using the Raman technique during nighttime (Ansmann et al., 1992) and the Klett/Fernald inversion technique during daytime (Klett, 1981, 1985; Fernald, 1984).

The relative errors of the aerosol backscatter (β_{aer}) and extinction (α_{aer}) coefficients and of the lidar ratio (LR = α_{aer}/β_{aer}) are mainly due to the presence of noise on the received lidar signal. Additionally, the lidar backscatter profile must be calibrated at a reference height region with negligible aerosol scattering (only Rayleigh scattering). This uncertainty in the calibration region in the clean upper free troposphere (at 532 and 1064 nm) may lead to further errors. Finally, by applying Gaussian's law of error propagation and assuming reasonable uncertainties at the input parameters mentioned above and the lidar overlap function assumed, the remaining systematic uncertainties are of the order of 5–15% on the β_{aer} and of 10–25% on the α_{aer} (Ansmann et al., 1992; Mattis et al., 2002). Therefore, the systematic uncertainty on the lidar ratio is of the order of 5–10%. Furthermore, the Turkish lidar is equipped with polarization sensitive channels at 355 nm. Prior to presenting the aerosol profiles obtained by the three lidars, we have to mention that the full overlap distances (Wandinger and Ansmann, 2002) of the operating lidars are: 900 m (in Athens), 1200 m (in Thessaloniki) and 800 m (in Turkey) (Table 1).

2.2. FLEXPART dispersion model

To simulate the ash transport, we employed the Lagrangian particle dispersion model FLEXPART (Stohl et al., 1998, 2005). FLEXPART traces a large number of virtual particles that follow the mean winds with superimposed random motions representing turbulence and convection. Sedimentation, dry and wet deposition of the particles was also considered. The model was driven here by operational analysis data from the European Centre for Medium-Range Weather Forecasts (ECMWF) model at a horizontal resolution of 0.18° × 0.18° and 91 vertical model levels. The output resolution was set to 0.25° × 0.25° horizontally, and 38 vertical levels with 250 m resolution.

The ash emission strength was determined by an inversion algorithm (Stohl et al., 2011) which uses satellite data to constrain modeled ash emissions. The simulation releases 21 million particles from the volcano, binned in 25 particle size classes between 0.25 and 250 μm diameters. Only "fine" ash particles (diameter up to 20 μm) can reach the lidar stations after several days of advection, while larger ash particles mostly fall out by gravitational settling before reaching the stations. More information on FLEXPART can be found at http://transport.nilu.no/flexpartand the model results used here are described in detail in Stohl et al. (2011).

2.3. The BSC-DREAM8b dust model

The dust forecast is based on the operational outputs (aerosol dust load) of the BSC-DREAM8b (operated in Barcelona, Spain: http://www.bsc.es/projects/earthscience/DREAM/) model (Nickovic et al., 2001; Pérez et al., 2006). The model simulates or predicts the 3-dimensional field of the dust concentration in the troposphere. The dust model takes into account all major processes of dust life cycle, such as dust production, horizontal and vertical diffusion and advection and wet and dry deposition. The model also includes the effects of the particle size distribution on aerosol dispersion. In this version of the model the dust mass is described by particles with four sizes, resulting from the structure of desert soils based on the content of clay, small silt, large silt and sand. The resolution of the model is set to 50 km in the horizontal and to 15 km in the vertical. Recently, BSC-DREAM8b was coupled to the combined photochemical forecast MM5-EMEP-CMAQ modeling system to provide an integrated air quality model with remarkable improvement in the discrete and skill-scores evaluation of particulate matter less than 10 μm effective

Table 1
Raman lidar stations, their geographical coordinates and location, the wavelengths, and aerosol retrieval methods used.

Lidar station	Latitude (°), Longitude (°)	Station altitude/Full overlap (a.s.l. m)	Wavelengths used (nm)	Aerosol retrieval method
Athens-GR	37.97N, 23.79E	200/900	355/387/407/532/607/1064	Raman/Klett/Fernald
Thessaloniki-GR	40.51N, 22.93E	40/1200	355/387/532/607	Raman/Klett/Fernald
Istanbul-TU	40.8N, 29.43E	170/800	355/387/407/532/607/1064	Raman/Klett/Fernald

diameter (PM_{10}) exceedances in the Iberian Peninsula (Jiménez-Guerrero et al., 2008).

2.4. The HYSPLIT dispersion model

HYSPLIT (version 4.9) is a system for computing trajectories and dispersion using either a puff or particle approach (Draxler et al., 2009). HYSPLIT is a Lagrangian dispersion model that relies on meteorological data to drive the simulations. The HYSPLIT model was used to calculate three-dimensional 7- to 13-day back-trajectories using 3-hourly archive meteorological data from the National Weather Service's National Centers for Environmental Prediction (NCEP) from the Global Data Assimilation Group (GDAS).

3. Results and discussion

Fig. 1 shows total columnar concentrations of volcanic ash (in mg m^{-2}) according to FLEXPART simulations, for the period between May 10 and May 21, 2010 at 12:00 Universal Time Constant (UTC). The three considered lidar stations (Athens–Thessaloniki–Istanbul), are denoted by colored circles (Athens: black, Thessaloniki: blue, Istanbul: red), while the position of the Eyjafjallajökull volcano is shown by a red triangle. From May 10 to 12 the main volcanic ash cloud was transported South-Southwestward to the Atlantic Ocean, the Iberian Peninsula, Southern France and Northern Italy, before reaching the Eastern Mediterranean area where the total columns of ash remained smaller than 300 mg m^{-2}. Later, on May 13–16 the volcanic cloud passed over South-western Europe (May 13), then over Southern Italy and the Eastern Mediterranean (May 14) and then again new ash clouds reached the UK, passed over the Iberian Peninsula (May 15) and, finally, on May 16 reached again the Balkans area. The ash cloud was transported over the North Sea on 17–18 May (Stohl et al., 2011) where high ash concentrations were sampled by a research aircraft (Schumann et al., 2011).

A substantial part of the ash cloud was subsequently transported over Central Europe (May 18) and then moved over South, South-Eastern Europe and the Balkans area, finally fading out (May

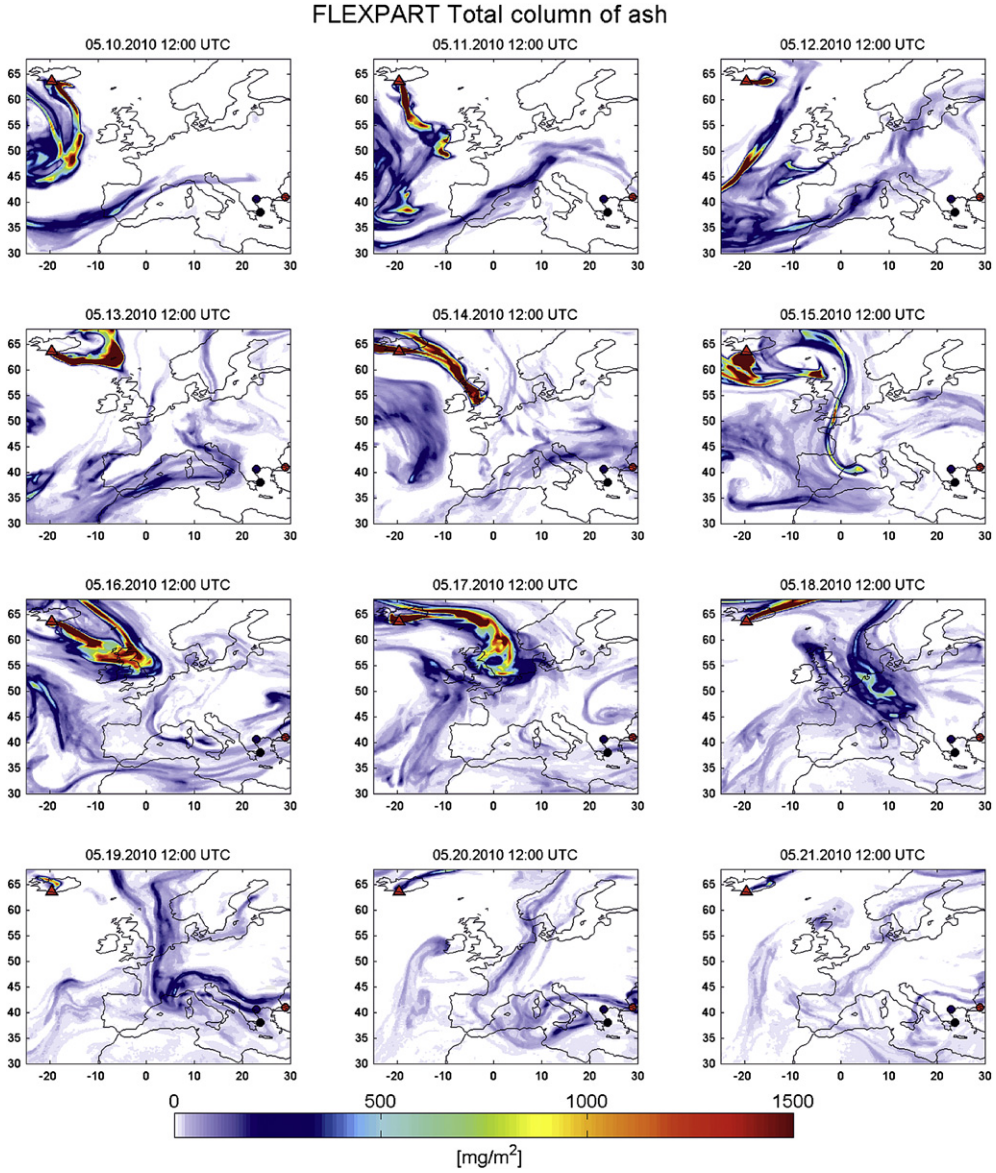

Fig. 1. FLEXPART simulations of the Eyjafjallajökull volcanic ash (total column in mg m^{-2} for all 25 particle size classes) for the period of May 10–21, 2010 (12:00 UTC). The positions of the lidar stations are marked with colored circles: Athens (black), Thessaloniki (blue), Istanbul (red).

19–21). To summarize, Greece was mainly affected by ash clouds between May 14 and 20, while traces of ash particles were observed also on May 10. Turkey was mostly affected on May 14, 16–17, and between May 19 and 21.

In Fig. 2, sunphotometric columnar measurements are presented from AERONET stations close to the lidar measurements that will be presented in the following. Specifically, time series of the total Aerosol Optical Depth (AOD) along with the fine and coarse mode contribution and the Ångström Exponent (AE) are presented for each site (upper panels). In the lower panels of Fig. 2, FLEXPART columnar concentrations are plotted to denote ash presence over the sites (black lines) along with BSC-DREAM8b model simulations to depict the Saharan dust columnar concentrations (ochre lines).

In Fig. 2(a), sunphotometric data from the closest to Istanbul AERONET station (Xanthi, Greece: 41°N 214°E, which is 380 km from Istanbul and at about the same latitude) are presented, for the period between May 10 and 21. The columnar AOD at 500 nm shows strong variability. The maximum values of the AOD (of the order of 0.3) were found on May 12, 13 and 20. The coarse mode contribution to the total AOD reaches the maximum values on May 12 and 13, due to presence of Saharan dust over the site. This is evident from the lower panel of Fig. 2(a), where the FLEXPART and BSC-DREAM8b model simulations of the columnar concentrations of ash and dust are presented, respectively. Saharan dust had strong impact also on the AE values (of the order of 0.5) on May 12 and 13. The lidar measurements for Istanbul are presented only for May 20, since is a newly developed system. On that day, according to FLEXPART, ash particles were advected over Istanbul, however, no clear ash signature is visible on the sunphotometric measurements over Xanthi. Specifically, the AE found equal to 1.3 indicating the presence of small particles, while the coarse mode contribution to the total AOD was found equal to 14%.

In Fig. 2(b), AERONET data for Athens are presented for the period between May 10 and 21. Maximum values of AOD at 550 nm (of the order of 0.4) were found on May 12, 13 and 15. The dust presence according to BSC-DREAM8b has a clear impact on sunphotometric data between May 12 and 15 (large AODs accompanied with small AE values). On May 19, when Raman lidar measurements are available for Athens, ash particles are present according to FLEXPART, while no dust from Saharan is forecasted by BSC-DREAM8b. Similar to the Xanthi station, sunphotometric columnar AE values ($\sim$1.5) and coarse contribution to the total AOD (27%) are not indicative of the ash presence over Athens.

Raman lidar measurements over Thessaloniki are available for May 10. According to model simulations on that day (Fig. 2(c) – lower panel), ash particles are advected along with dust particles from Saharan desert. Small AODs were then observed ($\sim$0.1) with high AE values ($\sim$1.3) which again, are not indicative of the presence of coarse particles.

To summarize, AERONET columnar measurements did not indicate ash presence over the studies areas, since the large ash particles were expected to increase the coarse mode contribution to the total AOD, leading to small AE values. Similarly, AERONET measurements over Germany depicted AE values for ash from Eyjafjallajökull of the order of 0.35–1.5 (Ansmann et al., 2010, 2011; Wiegner et al., 2011), both for the short wavelength range (AE 380/500 nm) and for the long wavelength range (AE 500/1640 nm) during the maximum ash load. However, columnar effective AEs are not representative of the ash layers, since the Planetary Boundary Layer (PBL) aerosol burden is contaminated by local urban pollution sources. This is especially true for the sites examined here (Athens, Thessaloniki, Istanbul), which are considered as the major hot spots of urban air pollution in the East Mediterranean (e.g. Kanakidou et al., 2010). Considering also the small columnar concentrations of ash particles over Eastern Mediterranean, as simulated by FLEXPART, only lidar instruments are capable of providing direct information on the ash presence in the vertical direction.

To define the ash layers over the three lidar stations, we followed certain criteria that will be presented in the following, concerning the depolarization ratio (available only for the Istanbul site) and the extinction or backscatter-related AE (BRAE and ERAE, respectively), which is indicative of the size of aerosol particles. After the definition of the ash layers, the center of mass height, z_c, for each layer has been calculated, following the definition given in Mona et al. (2006). Specifically, the height of the center of mass is estimated by the calculation of the backscatter weighted altitude (z_c) given as follows, where β represents the aerosol backscatter coefficient:

$$z_c = \frac{\int_{z_b}^{z_t} z \cdot \beta(z) dz}{\int_{z_b}^{z_t} \beta(z) dz} \quad (1)$$

The backscatter weighted altitude is an approximation of the centre of mass of the aerosol layer that exactly coincides with the true center of mass if both composition and size distribution of the particles are constant with altitude. Thus, the estimate of the center of mass gives us information about the altitude where the most relevant part of the aerosol load is located (Mona et al., 2006).

The heights of center of the mass calculated for the three lidar stations (3.2 km for Athens and Thessaloniki and 2.2 km for Istanbul) were considered as arrival heights for the back-trajectory analysis presented in Fig. 3. Specifically, 7-day backward trajectories were calculated using HYSPLIT code (Fig. 3) for the arrival heights previously mentioned and for the specific measurement time of each lidar profile (Istanbul: May 21, 03:00 UTC and Athens: May 19, 18:00 UTC; especially for Thessaloniki 13-days trajectories were considered, ending on May 10, 18:00 UTC). From Fig. 3 it is evident that the air masses ending over Istanbul (red line/asterisks) at 2.2 km on May 21 (at 02:00 UTC), originated about 100–300 km south of Iceland 6–7 days ago from heights around 6–7 km, which is consistent with the height range of the emitted ash (Stohl et al., 2011; Colette et al., 2011), as well as with the FLEXPART simulations (Fig. 1).

The air masses observed over Athens (black line/squares) on May 19 at 18:00 UTC around 3.2 km height, originated from the 7–8 km height region southern of Iceland some 5 days before. This is again consistent, as previously, with the height range of the emitted ash, as well as with the FLEXPART simulations (Fig. 1). Finally, for the case of Thessaloniki (blue line/crosses), the air masses observed on May 10 at 18:00 UTC around 3.2 km height originated from Iceland some 13 days before, starting at heights around 5 km. Later they passed over the Saharan desert at low altitudes (less than 100 m a.s.l.) some 72 h prior to their arrival over Thessaloniki. While passing over the desert area, the air masses were enriched with mineral dust aerosols, thus mixing of ash and dust should be observed. Thus, air mass back-trajectory simulations indicate clearly that aged ash particles of the order of 5–6 days arrived over Athens and Istanbul. However, for Thessaloniki, the air masses passed also over the Saharan desert area resulting in a mixture of dust and ash particles. Beyond the back-trajectory simulations, this argument is also supported by FLEXPART and BSC-DREAM8b simulations, as already presented in Fig. 2.

To characterize the vertical extent of the ash layers and the optical properties of the aged ash particles, we will refer to the aerosol vertical profiles obtained by the three Raman lidar systems. The Raman lidar measurements for the three sites of our study are presented in Fig. 4. The first four panels present the profiles of the aerosol optical properties retrieved, namely the extinction

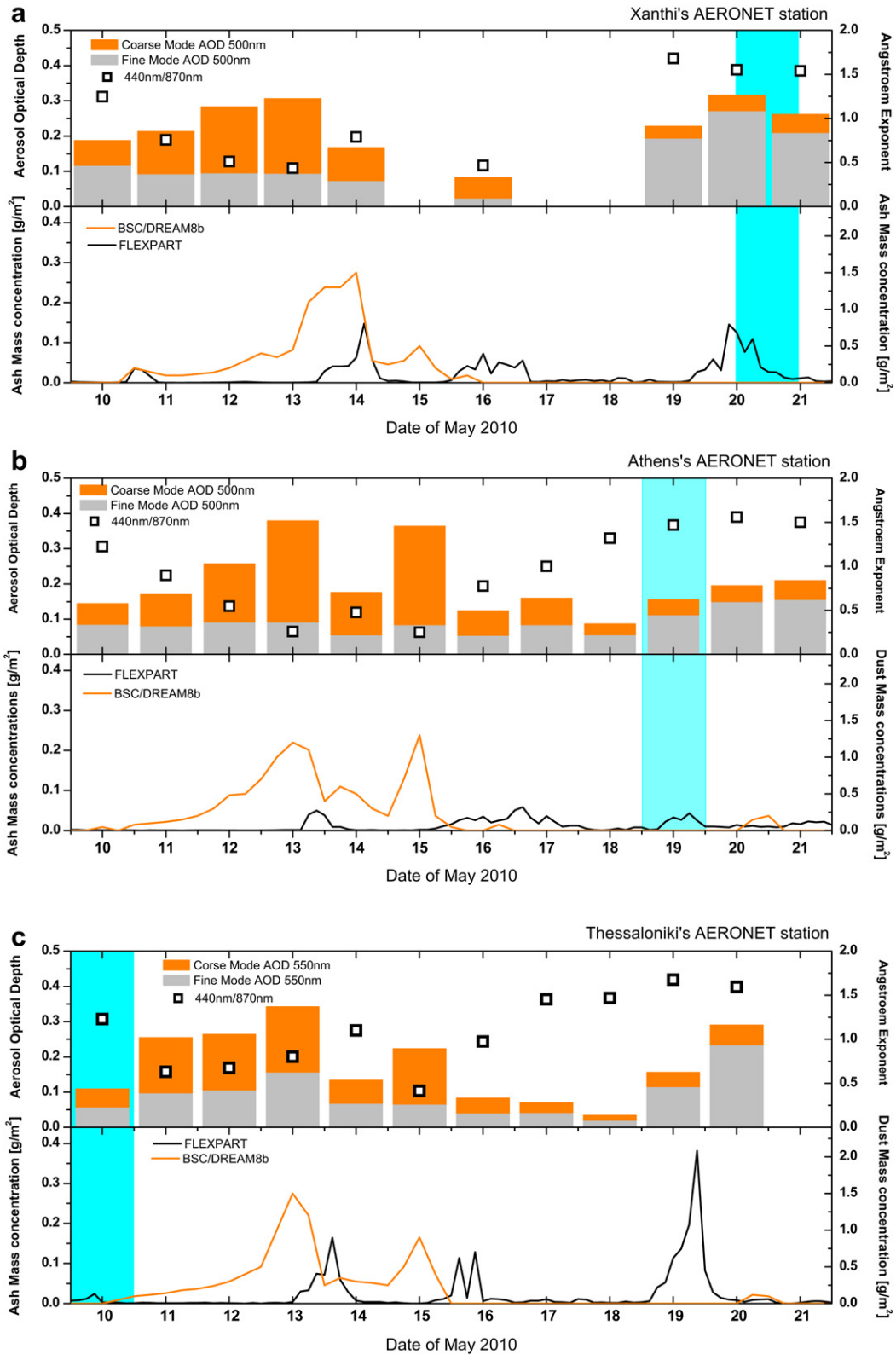

Fig. 2. AERONET fine/coarse mode AOD at 550 nm for the period between May 10 and 21 and the AE of 480 nm/870 nm retrievals (upper graph) and temporal evolution of the ash columnar concentration (ACC) (in g m^{-2}, for ash particles up to 10 μm) according to FLEXPART simulations and temporal evolution of the dust columnar concentration (DCC) (in g m^{-2}) according to BSC-DREAM8b simulations for the three considered lidar stations (a) Istanbul, (b) Athens and (c) Thessaloniki from May 10 to 21, 2010. The blue columns highlight the selected days for further analysis. (For interpretation of the references to color in this figure legend, the reader is referred to the web version of this article.)

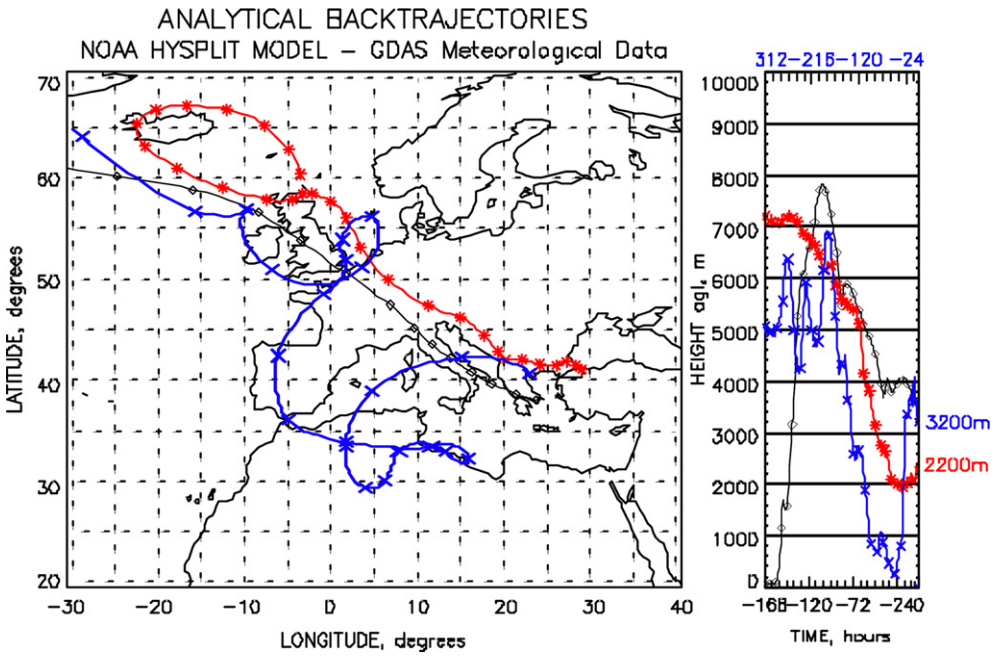

Fig. 3. Back-trajectories of air masses ending at the heights of center of mass over Athens (May 19, 2010 at 18:00 UTC, 7-days) at 3200 m (black line/squares), Thessaloniki (May 10, 2010 at 18:00 UTC, 13-days) at 3200 m (blue line/crosses), and Istanbul (May 20, 2010 at 03:00 UTC, 7-days) at 2.2 km (red line/asterisks) using the HYSPLIT model. (For interpretation of the references to color in this figure legend, the reader is referred to the web version of this article.)

coefficient, the backscatter coefficient, the lidar ratio and the BRAE or ERAE, respectively. In the fifth panel, the vertical profiles of ash and dust concentrations over the sites are also presented according to FLEXPART and BSC-DREAM8b models, respectively. The ochre shaded area represents the PBL height, as this has been calculated by radiosonde data taken by nearby to the lidar sites meteorological stations.

In Fig. 4(a), the measurements in Istanbul are first presented. For this station, the depolarization ratio profile at 355 nm is available and presented in the fourth panel along with the BRAE. The particle linear depolarization ratio observed over Istanbul at 355 nm during May 21 after 02:00 UTC is stronger between 2 and 3 km height (ranging from 10 to 25%, which is a clear indication of non-spherical particles) than below 2 km, where it stays below 5% (nearly spherical particles). The particle linear depolarization ratios measured (10–25%), were lower than those measured a few days after the on-set of the Eyjafjallajökull eruption in April 2010, in another, denser ash cloud (around 35–40% at 355 and 532 nm) over Germany and France (Ansmann et al., 2010, 2011; Miffre et al., 2010; Gasteiger et al., 2011; Gross et al., 2011; Miffre et al., 2011; Wiegner et al., 2011). In absence of dust particles over Istanbul, these data indicate clearly the presence of non-spherical particles from other source that a desert. This is also revealed from aerosol depolarization observations of CALIPSO over Istanbul on the same day (not shown here, but available at: http://eosweb.larc.nasa.gov/PRODOCS/calipso/table_calipso.html).

The smaller depolarization ratios measured over Turkey, than over Germany indicate that the aged ash particles probed over Istanbul are more spherical, which can result from possible humidity uptake (Lathem et al., 2011) or removal of greater particles with more complicated non-spherical shapes. Other possible processes that could lead to the reduction of depolarization ratio values are the formation of spherical sulphate in the ash-dominated layers and the mixing with anthropogenic aerosol (urban haze) (Miffre et al., 2011). However, the humidity uptake is considered here as the major reason, since the BRAE vertical profile presented along with the depolarization, shows values between 0 and 1 (with a mean value of 0.4 ± 0.4), indicating the presence of rather large particles in the layer between 2 and 3 km (denoted with gray color). The AERONET columnar value of the ERAE for the same day was found equal to 1.3 which is consistent with the average derived from the lidar measurements (~ 1.1). The presence of ash is additionally indicated in these altitudes by the FLEXPART concentration profile (black line/squares), while the dust presence is excluded according to BSC-DREAM8b concentration profile (ochre line/circles).

Therefore, concerning the Greek lidar stations, and since these do not operate depolarization channels, the ash layers over these sites are assumed in the ranges where the AEs are between 0 and 1, when these layers are accompanied with FLEXPART model simulations. Fig. 4(b) shows the aerosol optical properties obtained over Athens by the multi-wavelength Raman lidar on May 19 between 18:00 and 21:00 UTC. The corresponding ash mass concentration profile (in $\mu g\ m^{-3}$) simulated by the FLEXPART model (black line/squares) as well the dust mass concentration profile (in $\mu g\ m^{-3}$) simulated by the BSC-DREAM8b model (ochre line/circles) are shown in the right plot of the Figure. The simulated vertical concentration profiles show that the ash layer ranges from 3 up to 5 km and that no Saharan dust aerosols were present during the same time. Based on the BRAE and ERAE vertical profiles, as well as the FLEXPART concentration profile, the layer between 3 and 4.5 km is considered as ash layer.

The mean extinction-related as well the mean backscatter-related AE inside the layer remain below 1 reaching values of the order of 0.57 and 0.72, respectively. The mean values of the lidar ratio within the layer were found equal to 67 and 89 for ultraviolet and visible radiation, respectively. Those values are generally greater than the ones reported for volcanic ash (about 45–90 sr) (Ansmann et al., 2010; Gross et al., 2011; Wiegner et al., 2011) possibly due to the aging of the ash air masses examined here. The fine mode particle optical depth from AERONET measurements of 0.11 is comparable to the lidar derived boundary layer particle optical depth of about 0.10 at 532 nm (estimated from the 532 nm backscatter coefficient which is reliable down to low heights). The

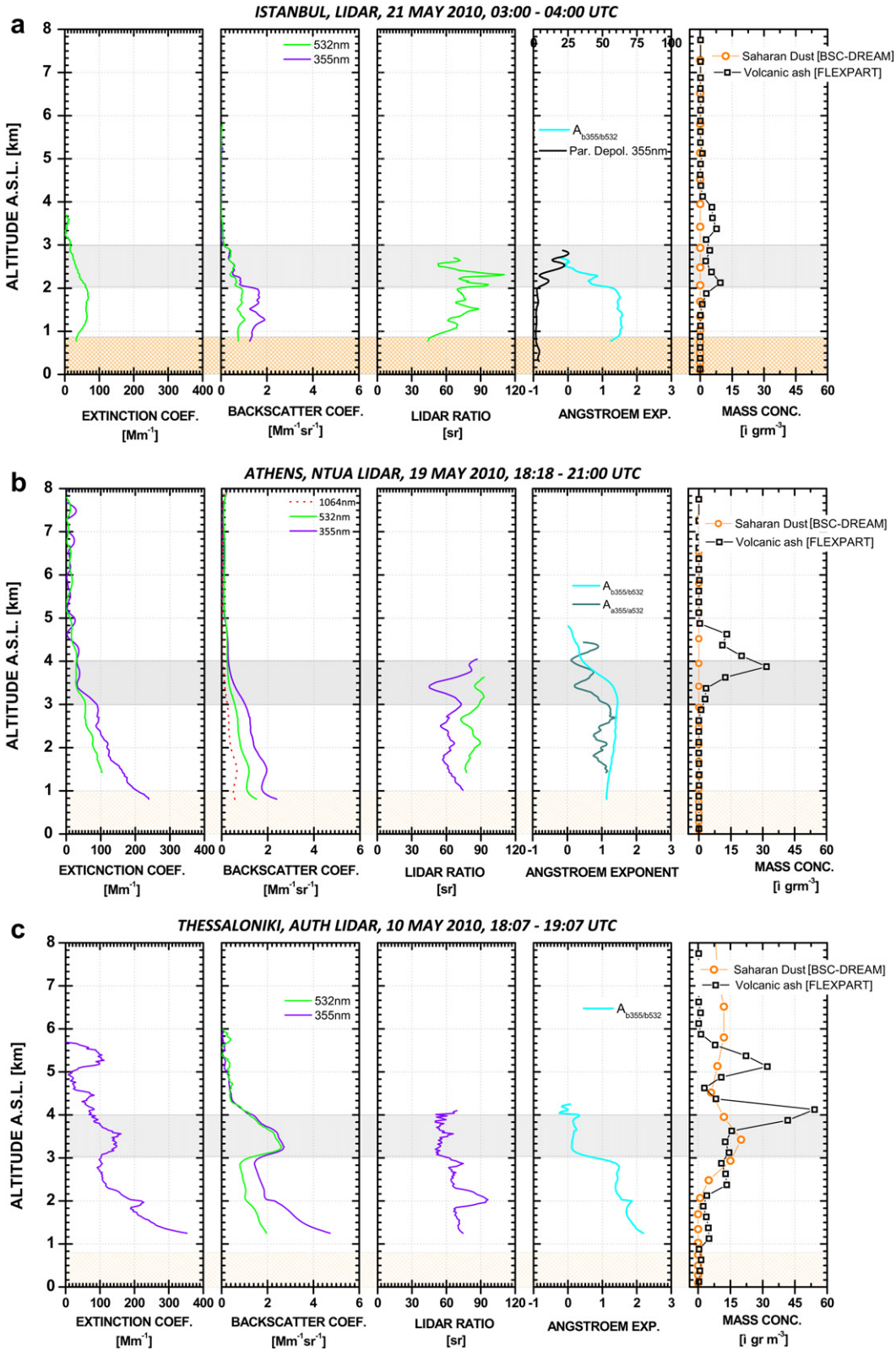

Fig. 4. Vertical extension of ash layers [top, base and thickness (in km)] and optical properties [aerosol extinction coefficient at 355 and/or 532 nm (in Mm^{-1}), aerosol backscatter coefficient at 355 and/or 532 nm (in $Mm^{-1}\ sr^{-1}$), lidar ratio at 355 and/or 532 nm, extinction and/or backscatter-related Ångström exponent (355 nm/532 nm) and depolarization ratio at 355 nm (%) (only for Istanbul's case)] of ash particles over (a) Istanbul (May 21) (b) Athens (May 19), (c) Thessaloniki (May 10), as retrieved by lidar measurements (right plot). Vertical distribution of the ash concentration (in $\mu g\ m^{-3}$, for ash particles up to 10 μm) simulated by FLEXPART model (black line/squares) and the dust concentration simulated by the BSC-DREAM8b model (ochre line/circles). (For interpretation of the references to color in this figure legend, the reader is referred to the web version of this article.)

Table 2
Mean aerosol properties, measured in the ash layer (located at the indicated height range) during nighttime over the Raman lidar stations (Athens, Thessaloniki, Istanbul): AOD (355 nm), AOD (532 nm), LR (355 nm) and LR (532 nm).

Station	Date	Height range (km)	AOD 355 nm	AOD 532 nm	LR (sr) 355 nm	LR (sr) 532 nm	A_{ap}	A_{bsc}	Dep. [%] 355 nm
Athens	19/05/10 21:00 UT	3.0–4.8	0.06	0.05	67 ± 13	89 ± 3	0.57 ± 0.26	0.72 ± 0.49	N/A
Thessaloniki	10/05/10 18:30 UT	3.0–4.0	0.12	N/A	55 ± 4	N/A	N/A	0.19 ± 0.09	N/A
Istanbul	21/05/10 03:00 UT	2.0–3.0	N/A	0.03	76 ± 15	N/A	N/A	0.4 ± 0.4	14 ± 7

N/A: Non applicable.

coarse-mode-related optical depth of 0.04 at 500 nm in Fig. 2(b) can be interpreted as the ash-related optical depth.

This value is also in good agreement with the lidar optical depth for the ash layer (equal to 0.04) observations. As a conclusion, lidar measurements indicate that the coarse particles are located in the layer defined by our criteria and furthermore that the AOD within this layer agrees with sunphotometric retrievals of the coarse mode. For the specific time period no presence of Saharan dust aerosols was predicted by the BSC-DREAM8b model.

Fig. 4(c) shows the Raman lidar retrievals for Thessaloniki's station on May 10 between 18:07 and 19:07 UTC. From the vertical profiles of the aerosol optical properties a strong layer was observed between 3 and 4 km. The corresponding ash mass concentration profile (in μg m^{-3}) simulated by the FLEXPART model (black line/squares) as well the dust mass concentration profile (in μg m^{-3}) simulated by the BSC-DREAM8b model (ochre line/circles) are shown in the right hand side of that Figure. Thus, the simulated vertical concentration profiles show ash layers at height ranges from 1 to 6 km (with peaks at 4 and 5 km) and also Saharan dust aerosols between 2 and 8 km (with peaks at 3.5 and 6 km). The mass concentration from both models was up to 20 μg m^{-3} for mineral dust and up to 30 and 56 μg m^{-3} for the volcanic ash particles.

Based on BRAE and ERAE vertical profiles, the aerosol layer between 3 and 4 km is considered here for further analysis. The mean BRAE value inside the layer dropped below 0.5 (0.19 ± 0.09), indicating the presence of rather coarse particles. The mean values of the LR within the layer were found almost constant and equal to 57 ± 4 sr at 355 nm, indicating good mixing of aerosols inside the layer. The retrieved optical properties of the particles over Thessaloniki are comparable with Athens's and Istanbul's ones, however in this case, dust and ash are possibly mixed, indicating a similar behavior of these aerosol types concerning their optical properties.

Table 2 summarizes the results from selected Raman lidar aerosol profiles which were used to provide typical mean values of the aerosol optical properties inside the ash layers over the three lidar stations: AOD at 355 nm and 532 nm (when available), as well as the LR at 355 nm and 532 nm. The ash layer thickness typically ranged between 1 and 2 km, while its top and base ranged between 2 and 5, respectively, in accordance with Dacre et al. (2011), Kaminski et al. (in press) and Stohl et al. (2011). The largest aerosol backscatter values at 532 nm (2.06 ± 0.43 Mm^{-1} sr^{-1}) were observed over Thessaloniki, while the lowest ones over Athens (0.30 ± 0.09 Mm^{-1} sr^{-1}). These reported values on the aerosol backscatter coefficient are much lower than those reported over Germany during April 16, 2010 by Ansmann et al. (2010) and Ansmann et al. (2011).

The wavelength dependence of the aerosol backscatter coefficients provided BRAE values lower than 1 for all stations, consistent with observations by Ansmann et al. (2010) and Ansmann et al. (2011). We found that the AOD values inside the ash layers were quite low (0.12–0.06 at 355 nm and 0.05–0.03 at 532 nm). The corresponding LR values, for all lidar stations, were found to range between 55 and 67 sr at 355 nm and 76–89 sr at 532 nm, which are within the range of those reported (50–95 sr) for the same volcanic eruption on April 2010 by Ansmann et al. (2010, 2011) and Gross et al. (2011). The high values of the mean aerosol optical properties at Thessaloniki's station are mainly due to the presence as well of the dust aerosols during May 10 over the site. This can be supported by the extremely low BRAE values (0.19 ± 0.09) within the selected layer.

4. Conclusions

Volcanic ash-related vertical extension layer and aerosol optical properties were studied over three selected sites (Athens, Thessaloniki and Istanbul) in the Eastern Mediterranean region from May 10 to 21. Ash layers were observed in the height range between near ground (around 1.8 km) and 5–6 km, with thicknesses of the order of 1–2 km. The observed linear depolarization ratios of aged (6–7 days) volcanic ash particles was found to be of the order of 10–30%, which is smaller than the typical values of pure ash (35–40%) as recently reported during the April 2010 period over Germany and France (Ansmann et al., 2010, 2011; Miffre et al., 2010; Gasteiger et al., 2011). This fact indicates that ash non-sphericity becomes less with age. The AOD of the ash layer was found to range between 0.12–0.06 at 355 nm and 0.02–0.04 at 532 nm. The LR values inside the ash layers were found to range between 55–67 sr at 355 nm and 76–89 sr at 532 nm. The FLEXPART Lagrangian dispersion model was used to simulate the dispersion of ash particles over the European continent, along with the BSC-DREAM8b model for dust simulations. The optical properties of volcanic aerosols, as well as the vertical extension of ash layers (occasionally mixed dust), provided by synergy of lidars and models, as presented here, can be useful for studies of volcanic ash dispersion, as well as for aviation security agencies to avoid engine hazards.

Acknowledgments

This research has been co-financed by the European Union (European Social Fund – ESF) and Greek national funds through the Operational Program "Education and Lifelong Learning" of the National Strategic Reference Framework (NSRF) – Research Funding Program: Heracleitus II. Investing in knowledge society through the European Social Fund. The financial support of the EARLINET-ASOS Network by the European Commission under grant RICA-025991 is gratefully acknowledged. REM acknowledges the funding of the "Greek State Scholarship Foundation: IKY". The forecast of the dust transport model BSC-DREAM8b was provided by the Barcelona Supercomputing Center. Air masses back-trajectories were produced with the Hybrid Single-Particle Lagrangian Integrated Trajectory model (NOAA). The authors gratefully acknowledge the NOAA Air Resources Laboratory (ARL) for the provision of the HYSPLIT transport and dispersion model. The ESA financial support under ESTEC contract 21487/08/NL/HE is acknowledged. AS and NK have been supported by ESA in the framework of the SAVAA project. The Turkish team acknowledges support of the Turkish State Planning Committee (DPT). The authors are grateful to the two reviewers for their helpful comments and suggestions.

References

Allakhverdiev, K.R., Baykara, T.K., Bekbolet, M., Huseyinoglu, M.F., Ozbek, S., Salaeva, Z., Vartapedov, S., Veselovskii, I., 2009. New multiwavelength Mie-Raman lidar in Turkey for aerosol studies. In: Proceedings of the International Conference on Advanced Laser Physics, ALT'09, Antalya.

Ansmann, A., Riebesell, M., Wandinger, U., Wietkamp, C., Voss, E., Lahmann, W., Michaelis, W., 1992. Combined Raman elastic-backscatter lidar for vertical profiling of moisture. Aerosol extinction, backscatter, and lidar ratio. Applied Physics B55, 18–28.

Ansmann, A., Tesche, M., Groß, S., Freudenthaler, V., Seifert, P., Hiebsch, A., Schmidt, J., Wandinger, U., Mattis, I., Müller, D., Wiegner, M., 2010. The 16 April 2010 major volcanic ash plume over central Europe: EARLINET lidar and AERONET photometer observations at Leipzig and Munich, Germany. Geophysical Research Letters 37, L13810. doi:10.1029/2010GL043809.

Ansmann, A., Tesche, M., Seifert, P., Groß, S., Freudenthaler, V., Apituley, A., Wilson, K.M., Serikov, I., Linné, H., Heinold, B., Hiebsch, A., Schnell, F., Schmidt, J., Mattis, I., Wandinger, U., Wiegner, M., 2011. Ash and fine mode particle mass profiles from EARLINET–AERONET observations over central Europe after the eruptions of the Eyjafjallajökull volcano in 2010. Journal of Geophysical Research 116, D00U02. doi:10.1029/2010JD015567.

Bitar, L., Duck, T.J., Kristiansen, N.I., Stohl, A., Beauchamp, S., 2010. Lidar observations of Kasatochi volcano aerosols in the troposphere and stratosphere. Journal of Geophysical Research 115, D00L13. doi:10.1029/2009JD013650.

Bösenberg, J., et al., 2003. EARLINET: A European Aerosol Research Lidar Network. MPI Report 348. Max-Planck-Institut für Meteorologie, Hamburg, Germany.

Colette, A., Favez, O., Meleux, F., Chiappini, L., Haeffelin, M., Morille, Y., Malherbe, L., Papin, A., Bessagnet, B., Menut, L., Leoz, E., Rouïl, L., 2011. Assessing in near real time the impact of the April 2010 Eyjafjallajökull ash plume on air quality. Atmospheric Environment 45, 1217–1221.

Corradini, S., Merucci, L., Prata, A.J., Piscini, A., 2010. Volcanic ash and SO_2 in the 2008 Kasatochi eruption: retrievals comparison from different IR satellite sensors. Journal of Geophysical Research 115, D00L21. doi:10.1029/2009JD013634.

Dacre, H.F., Grant, A.L.M., Hogan, R.J., Belcher, S.E., Thomson, D.J., Devenish, B.J., Marenco, F., Hort, M.C., Haywood, J.M., Ansmann, A., Mattis, I., Clarisse, L., 2011. Evaluating the structure and magnitude of the ash plume during the initial phase of the 2010 Eyjafjallajökull eruption using lidar observations and NAME simulations. Journal of Geophysical Research 116, D00U03. doi:10.1029/2011JD015608.

Davies, S., Larsen, G., Wastegård, S., Turney, C.S.M., Hall, V.A., Coyle, L., Thordarson, T., 2010. Widespread dispersal of Icelandic tephra: how does the Eyjafjöll eruption of 2010 compares with past Icelandic events? Journal of Quaternary Science 25, 605–611.

Devenish, B.J., Thomson, D.J., Marenco, F., Leadbetter, S.J., Ricketts, H., Dacre, H.F., 2011. A study of the arrival over the United Kingdom in April 2010 of the Eyjafjallajökull ash cloud using ground-based lidar and numerical simulations. Atmospheric Environment 48, 152–164.

Draxler, R.R., Stunder, B., Rolph, G., Talylor, A.D., 2009. Hysplit 4 User's Guide. NOAA Air Resources Laboratory, Silver Spring, MD, USA.

Fernald, F.G., 1984. Analysis of atmospheric lidar observations: some comments. Applied Optics 23, 652–653.

Flentje, H., Claude, H., Elste, T., Gilge, S., Köhler, U., Plass-Dülmer, C., Steinbrecht, W., Thomas, W., Werner, A., Fricke, W., 2010. The Eyjafjallajökull eruption in April 2010 – detection of volcanic plume using in-situ measurements, ozone sondes and lidar-ceilometer profiles. Atmospheric Chemistry and Physics 10, 10085–10092.

Gasteiger, J., Groß, S., Freudenthaler, V., Wiegner, M., 2011. Volcanic ash from Iceland over Munich: mass concentration retrieved from ground-based remote sensing measurements. Atmospheric Chemistry and Physics 11, 2209–2223. doi:10.5194/acp-11-2209-2011.

Giannakaki, E., Balis, D.S., Amiridis, V., Zerefos, C., 2010. Optical properties of different aerosol types: seven years of combined Raman-elastic backscatter measurements in Thessaloniki, Greece. Atmospheric Measurement Techniques 3, 569–578.

Gross, S., Freudenthaler, V., Wiegner, M., Gasteiger, J., Geiss, A., Schnell, F., 2011. Dual-wavelength linear depolarization ratio of volcanic aerosols: lidar measurements of the Eyjafjallajokull plume over Maisach, Germany. Atmospheric Environment 48, 85–96.

Gudmundsson, M.T., Pedersen, R., Vogfjörd, K., Thorbjarnardóttir, B., Jakobsdóttir, S., Roberts, M.J., 2010. Eruptions of Eyjafjallajökull volcano, Iceland. EOS Transactions American Geophysical Union 91, 190–191.

Hoffmann, A., Ritter, C., Stock, M., Maturilli, M., Eckhardt, S., Herber, A., Neuber, R., 2010. Lidar measurements of the Kasatochi aerosol plume in August and September 2008 in Ny-Ålesund, Spitsbergen. Journal of Geophysical Research 115, D00L12. doi:10.1029/2009JD013039.

Jiménez-Guerrero, P., Pérez, C., Jobra, O., Baldasano, J., 2008. Contribution of Saharan dust in an integrated air quality system and its on-line assessment. Geophysical Research Letters 35, L03814. doi:10.1029/2007GL031580.

Kaminski, E., Tait, S., Ferrucci F., Martet, M., Hirn, B., Husson, P., 2011. Estimation of ash injection in the atmosphere by basaltic volcanic plumes: the case of the Eyjafjallajökull 2010 eruption. Journal of Geophysical Research, doi:10.1029/2011JB008297, in press.

Kanakidou, M., Mihalopoulos, N., Kindap, T., Im, U., Vrekoussis, M., Gerasopoulos, E., Dermitzaki, E., Unal, A., Koçak, M., Markakis, K., Melas, D., Kouvarakis, G., Youssef, A.F., Richter, A., Hatzianastassiou, N., Hilboll, A., Ebojie, F., Wittrock, F., von Savigny, C., Burrows, J.P., Ladstaetter-Weissenmayer, A., Moubasher, H., 2010. Megacities as hot spots of air pollution in the East Mediterranean. Atmospheric Environment 45, 1223–1235.

Karagulian, F., Clarisse, L., Clerbaux, C., Prata, A.J., Hurtmans, D., Coheur, P.F., 2010. Detection of volcanic SO_2, ash, and H_2SO_4 using the Infrared Atmospheric Sounding Interferometer (IASI). Journal of Geophysical Research 115, D00L02. doi:10.1029/2009JD012786.

Klett, J., 1981. Stable analytical inversion for processing lidar returns. Applied Optics 20, 211–220.

Klett, J., 1985. Lidar Inversion with variable backscatter extinction ratios. Applied Optics 24, 1638–1643.

Lathem, T.L., Kumar, P., Nenes, A., Dufek, J., Sokolik, I.N., Trail, M., Russell, A., 2011. Hygroscopic properties of volcanic ash. Geophysical Research Letters 38, L11802. doi:10.1029/2011GL047298.

Lettino, A., Caggiano, R., Fiore, S., Macchiato, M., Sabia, S., Trippetta, S., 2011. Eyjafjallajökull volcanic ash in southern Italy. Atmospheric Environment 48, 97–103.

Mamouri, R.E., Amiridis, V., Papayannis, A., Giannakaki, E., Tsaknakis, G., Balis, D., 2009. Validation of CALIPSO space-borne derived attenuated backscatter coefficient profiles using a ground-based lidar in Athens. Greece Atmospheric Measurements and Techniques 2, 513–522.

Markowicz, K.M., Zielinski, T., Pietruczuk, A., Posyniak, M., Zawadzka, O., Makuch, P., Stachlewska, I.S., Jagodnicka, A.K., Petelski, T., Kumala, W., Sobolewski, P., Stacewicz, T., 2012. Remote sensing measurements of the volcanic ash plume over Poland in April 2010. Atmospheric Environment 48, 66–75.

Matthias, V., Aulinger, A., Bieser, J., Cuesta, J., Geyer, B., Langmann, Bärbel, Serikov, I., Mattis, I., Minikin, A., Mona, L., Quante, M., Schumann, U., Weinzierl, B., 2012. The ash dispersion over Europe during the Eyjafjallajökull eruption – comparison of CMAQ simulations to remote sensing and air-borne in-situ observations. Atmospheric Environment 48, 184–194.

Mattis, I., Ansmann, A., Müller, D., Wandinger, U., Althausen, D., 2002. Dual-wavelength Raman lidar observations of the extinction-to-backscatter ratio of Saharan dust. Geophysical Research Letters 29, 1306. doi:10.1029/2002GL014721.

Mattis, I., Siefert, P., Müller, D., Tesche, M., Hiebsch, A., Kanitz, T., Schmidt, J., Finger, F., Wandinger, U., Ansmann, A., 2010. Volcanic aerosol layers observed with multiwavelength Raman lidar over central Europe in 2008–2009. Journal of Geophysical Research 115, D00L04. doi:10.1029/2009JD013472.

Miffre, A., David, G., Thomas, B., Rairoux, P., 2010. Characterization of Iceland volcanic aerosols by UV-polarization lidar at Lyon, SW Europe. In: Singh, U.N., Pappalardo, G. (Eds.), SPIE Proceedings, Lidar Technologies, Techniques, and Measurements for Atmospheric Remote Sensing VI, 7832, p. 78320Q. doi:10.1117/12.869019.

Miffre, A., David, G., Thomas, B., Rairoux, P., Fjaeraa, A.M., Kristiansen, N.I., Stohl, A., 2011. Volcanic aerosol optical properties and phase partitioning behavior after long-range advection characterized by UV-Lidar measurements, Atmospheric Environment, Corrected proof, Available online 20 April 2011. ISSN 1352–2310 48, 76–84.

Mona, L., Amodeo, A., Pandolfi, M., Pappalardo, G., 2006. Saharan dust intrusions in the Mediterranean area: three years of Raman lidar measurements. Journal of Geophysical Research 111, D16203. doi:10.1029/2005JD006569.

Nickovic, S., Kallos, G., Papadopoulos, A., Kakaliagou, O., 2001. A model for prediction of desert dust cycle in the atmosphere. Journal of Geophysical Research 106, 18113–18129.

Nicolae, D., Nemuc, A., Belegante, L., 2010. Mix of volcanic ash and Saharan dust over Romania, during Eyjafjallajökull eruption. In: Singh, U.N., Pappalardo, G. (Eds.), SPIE Proceedings, Lidar Technologies, Techniques, and Measurements for Atmospheric Remote Sensing VI, 7832, p. 78320N. doi:10.1117/12.869021.

Pérez, C., Nickovic, S., Pejanovic, G., Baldasano, J.M., Özsoy, E., 2006. Interactive dust-radiation modeling: a step to improve weather forecasts. Journal of Geophysical Research 111, D15214. doi:10.1029/2005JD006717.

Revuelta, M.A., Sastre, M., Fernández, A.J., Martín, L., García, R., Gómez-Moreno, F.J., Artíñano, B., Pujadas, M., Molero, F., 2011. Characterization of the Eyjafjallajökull volcanic plume over the Iberian Peninsula by lidar remote sensing and ground-level data collection. Atmospheric Environment 48, 46–55.

Sanderson, K., 2010. Out of the ashes. Nature 465, 544–545.

Schleicher, N., Kramar, U., Dietze, V., Kaminski, U., Norra, S., 2011. Geochemical characterization of single atmospheric particles from the Eyjafjallajökull volcano eruption event collected at ground-based sampling sites in Germany. Atmospheric Environment 48, 113–121.

Schumann, U., Weinzier, B., Reitebuch, O., Schlager, H., Minikin, A., Forster, C., Baumann, R., Sailer, T., Graf, K., Mannstein, H., Voigt, C., Rahm, S., Simmet, R., Scheibe, M., Lichtenstern, M., Stock, P., Rüba, H., Schäuble, D., Tafferner, A., Rautenhaus, M., Gerz, T., Ziereis, H., Krautstrunk, M., Mallaun, C., Gayet, J.-F., Lieke, K., Kandler, K., Ebert, M., Weinbruch, S., Stohl, A., Gasteiger, J., Olafsson, H., Sturm, K., 2011. Airborne observations of the Eyjafjalla volcano ash cloud over Europe during air space closure in April and May 2010. Atmospheric Chemistry and Physics 11, 2245–2279.

Seifert, P., Ansmann, A., Groß, S., Freudenthaler, V., Heinold, B., Hiebsch, A., Mattis, I., Schmidt, J., Schnell, F., Tesche, M., Wandinger, U., Wiegner, M., 2011. Ice formation in ash-influenced clouds after the eruption of the Eyjafjallajökull volcano in April 2010. Journal of Geophysical Research, doi:10.1029/2011JD015702.

Showstack, R., 2010. Eruptions of Eyjafjallajökull volcano, Iceland. EOS Transactions of the American Geophysical Union 91, 190–191.

Stohl, A., Hittenberger, M., Wotawa, G., 1998. Validation of the Lagrangian particle dispersion model FLEXPART against large scale tracer experiment data. Atmospheric Environment 32, 4245–4264.

Stohl, A., Forster, C., Frank, A., Seibert, P., Wotawa, G., 2005. Technical note: the Lagrangian particle dispersion model FLEXPART version 6.2. Atmospheric Chemistry and Physics 5, 2461–2474.

Stohl, A., Prata, A.J., Eckhardt, S., Clarisse, L., Durant, A., Henne, S., Kristiansen, N.I., Minikin, A., Schumann, U., Seibert, P., Stebel, K., Thomas, H.E., Thorsteinsson, T., Tørseth, K., Weinzierl, B., 2011. Determination of time- and height-resolved volcanic ash emissions for quantitative ash dispersion modeling: the 2010 Eyjafjallajökull eruption. Atmospheric Chemistry and Physics 11, 4333–4351. doi:10.5194/acp-11-4333-2011.

Wandinger, U., Ansmann, A., 2002. Experimental determination of the lidar overlap profile with Raman lidar. Applied Optics 41, 511–514.

Wiegner, M., Gasteiger, J., Groß, S., Schnell, F., Freudenthaler, V., Forkel, R., 2011. Characterization of the Eyjafjallajökull ash-plume: potential of lidar remote sensing. Journal of Physics and Chemistry of the Earth. doi:10.1016/j.pce.2011.01.006.